Scientific Research Publishing

Journal of Modern Physics, 2026, 17(4), 483-505
https://www.scirp.org/journal/jmp
ISSN Online: 2153-120X
ISSN Print: 2153-1196

Sources of Very High and Ultra High Energy Cosmic Ray Protons

Charles H. McGruder III

Department of Physics and Astronomy, Western Kentucky University, 1906 College Heights Blvd., Bowling Green, Kentucky, USA
Email: mcgruder@wku.edu

How to cite this paper: McGruder III, C.H. (2026) Sources of Very High and Ultra High Energy Cosmic Ray Protons. *Journal of Modern Physics*, **17**, 483-505.
https://doi.org/10.4236/jmp.2026.174022

Received: March 5, 2026
Accepted: April 24, 2026
Published: April 27, 2026

Abstract

We employ the theory of gravitational repulsion in the Schwarzschild field to show that neither Active Galactic Nuclei (AGN) nor main sequence stars are the sources of ultra high energy cosmic ray protons. Instead the theory leads to the conclusion that the sources of these particles are brown dwarfs except for protons with energies $>1.887\times10^{20}$ eV, which are produced by planetary mass bodies. The theory predicts that brown dwarfs and main sequence stars are the sources of very high energy cosmic ray protons.

Keywords

Cosmic Ray Protons, General Relativity, Gravitational Repulsion, Schwarzschild Field

1. Introduction

There are two fundamental questions of astroparticle physics: 1) How are very high and ultra high energy cosmic ray particles accelerated to the enormous energies we observe? 2) What are the sources of very high and ultra high energy cosmic ray particles [1]-[6]?

These questions are particularly acute for ultra high energy cosmic rays, $E > 1\ \text{EeV}$ [7]-[12]. In [13] we answered these two questions for very high and ultra high energy neutrinos. In [14] we answered the first question for cosmic ray protons by showing that they are accelerated to the highest energy observed by gravitational repulsion in the Schwarzschild field. Here we answer the second fundamental question: What are the sources of very high and ultra high energy cosmic ray protons?

Current thinking is that ultra high energy cosmic ray protons are possibly produced by active galactic nuclei (AGN) [7] [15]-[18]. But this view lacks conclusive observational evidence [10] [19]-[22].

In addition to AGN the following sources are thought to be possible sources of ultra high energy protons. Starburst Galaxies [17] [23]-[27], Gamma Ray Bursts [7] [28]-[33], Galaxy Cluster Accretion Shocks [16] [34]-[39], Fast-Spinning Newborn Pulsars/Magnetars [40]-[45], Binary neutron star mergers [46]-[48] and Tidal Disruption Events [49]-[52].

One of the major reasons AGN are considered prime candidate sources is that their physical conditions permit acceleration mechanisms capable of producing protons to very high and ultra high energy. Shock acceleration, which is widely believed to power solar energetic particles to TeV energy [53]-[59], is also one of the leading mechanisms proposed for accelerating cosmic-ray protons to the highest observed energies (EeV) [18] [60]-[66].

Shock mechanisms have a number of requirements among them are: 1) sufficient magnetic field strength 2) large enough spatial extent 3) long enough shock lifetime 4) efficient particle scattering (5) favorable shock geometry 6) a hard, pre-accelerated seed population and 7) a fast, strong shock that is the energy gain per cycle must be large [63] [67] [68]. All of these conditions are rarely met in the sun and only during very intense coronal mass ejections (CME) and that is why the production of solar TeV protons is rare. In order to create energies up to EeV all of these conditions must be stronger, larger and longer than in the sun, which is the case in AGNs.

In contrast to the shock theory according to our theory of the acceleration of cosmic ray protons to very high and ultra high energy is achieved through gravitational acceleration, specifically via gravitational repulsion in the Schwarzschild field of the source.

2. Gravitational Repulsion in the Schwarzschild Field

Early in the twentieth century Droste [69]-[71] and independently Hilbert [72] [73] discovered that a particle in radial motion will experience gravitational repulsion in the Schwarzschild field, if its Schwarzschild velocity obeys the inequality:

$$\frac{\mathrm{d}r}{\mathrm{d}t} > \frac{1}{\sqrt{3}}\left(1-\frac{\alpha}{r}\right) \tag{1}$$

where α is the Schwarzschild radius:

$$\alpha = 2GM \tag{2}$$

and where M is the mass of the gravitating body, G is the gravitational constant and the speed of light, $c = 1$. See [74] for the details of the history of this discovery.

Thereafter, however, decades of debate and confusion ensued and it was not until 1982 that we were able to confirm the reality of this phenomenon by clarifying the difference between local and distant observers [75]. In 2017 we showed how gravitational repulsion is responsible for acceleration of cosmic ray protons to the highest energy observed and we predicted that neutrinos would also be accelerated to ultra high energy [14]. In 2025 this prediction was verified by the detection of KM3-230213A, an extragalactic ultra high energy neutrino with 2.2 × 10^{20} eV [76].

In [14] and reviewed in [13] we showed how a proton can be accelerated to the ultra high energy of 10^{20} eV via gravitational repulsion in the Schwarzschild field. In [13] we derived the following equation:

$$d = \frac{2GM}{c^2} n \tag{3}$$

M is the mass of the source of the cosmic ray particle, d the distance of the source from earth, c the speed of light and G the gravitational constant and n the distance of the source in Schwarzschild radii, whereby n is a function of the particle energy observed on earth. For a proton of $E = 10^{20}\ \text{eV}$ we found that $n = 2.27181 \times 10^{22}$ [13].

Equation 3 was derived from the relationship between the Schwarzschild radial coordinate, r and the Schwarzschild radius, α : $r = n\alpha = d$ and the expression for the Schwarzschild radius including the c^2 factor: $\alpha = \frac{2GM}{c^2}$.

Application of the Theory of Gravitational Repulsion in Various Circumstances

Before we close this section we point out that others have applied the concept of gravitational repulsion in various circumstances. Dickau, Kauffmann and Robertson employ it to solve the problem of the accelerating expansion of the universe (in preparation). [77] investigate gravitational repulsion in the Einstein-zero-mass scalar theory. [78] discuss gravitational repulsion in an expanding ball of dust. [79] considered gravitational repulsion in the Kerr–Newman anti-de Sitter spacetime. [80] looked into gravitational repulsion in the Reissner-Nordström and Schwarzschild spacetimes. [81] show that the emission of gravitational waves leads to a repulsive gravitational force that diminishes with time but never disappears. They speculate that the repulsive force may be related to the observed expansion of the Universe. [82] point out that gravitational repulsion could appear in satellite experiments with beams of relativistic particles subject to very precise time measurements. [83] points out that gravitational repulsion occurs in geodesics in a quash-spherical spacetime. [84] investigates a number of aspects of the phenomenon of gravitational repulsion in static sources of the Reissner–Nordström field. [85] study gravitational repulsion in the Kerr and Kerr-Newman fields.

3. The Sources of Ultra High Energy Cosmic Ray Protons

In this section we determine the sources of ultra high energy, $E \geq 10^{18}\ \text{eV}$, cosmic ray protons according to our theory of gravitational repulsion in the Schwarzschild field. We first explore if their sources are Active Galactic Nuclei (AGN), which are leading candidates.

3.1. Active Galactic Nuclei

We now ask whether according to our theory an AGN can be the source of an ultra high energy proton of $E = 10^{20}\ \text{eV}$. To accomplish this task we employ the above equation. On the right side of the equation the only unknown quantity is M, the mass of the supermassive black hole in the presumed AGN source. But, we do know the range of masses, which is: $10^{6} M_{\odot} \lesssim M_{\text{SMBH}} \lesssim 10^{10} M_{\odot}$ [86]-[96]. So we can calculate the minimum and maximum distance of an AGN, that could possibly be responsible for producing our ultra high energy proton of 10^{20} eV.

If the AGN mass is $10^{6} M_{\odot}$ then $d = 2.175 \times 10^{6}\ \text{Gpc}$. If the AGN mass is $10^{10} M_{\odot}$ then its distance is $d = 2.175 \times 10^{10}\ \text{Gpc}$. Both of these distances are far greater than the maximum distance such a ultra high energy proton can travel in intergalactic space, which is only 100 Mpc [16] [17] [97] [98]. This maximum distance is due to the Greisen–Zatsepin–Kuzmin (GZK) effect, whereby ultra high energy protons are transformed into pions by interactions with CMB photons [99]-[103]. We conclude: AGNs can not be the source of ultra high energy cosmic rays according to our theory.

3.2. Stellar Mass Objects

In [13] we concluded that blazars, which are a subset of AGN, can not be the source of ultra high energy neutrinos. Instead we concluded that stellar mass bodies must be the source of these particles. Now that we have shown that according to our theory AGN are also not the source of ultra high energy cosmic ray protons, we ask could stellar mass bodies be the source of these particles? Following the procedure in the previous section we calculate the minimum and maximum distance of stellar mass objects to see, if they fall under the GZK limit of 100 Mpc.

As in [13] we base our analysis on the following: 1) The exterior gravitational field of a spherically symmetric non rotating star is the Schwarzschild metric. 2) F to M spectral type stars emit sporadically high energy protons [104]-[107]. 3) Therefore the minimum mass of stellar mass bodies that emit high energy protons is the minimum mass of M stars: $0.075 M_{\odot}$ [108]-[110]. 4) The maximum mass of stellar mass bodies that emit high energy protons is the maximum mass of F stars: $1.7 M_{\odot}$ [111] [112].

Inserting the minimum mass of M stars of $0.075 M_{\odot}$ into the Equation (3) yields: 163.1 Mpc. Inserting the maximum mass of F stars: $1.7 M_{\odot}$ yields: 3696 Mpc. These values are larger than the GZK limit of 100 Mpc. Consequently, we conclude that main sequence stars can not be the source of ultra high energy protons.

3.3. Brown Dwarfs as the Source of Ultra High Energy Cosmic Ray Protons

Since we know the maximum distance of the source of ultra high energy cosmic ray protons, $d = 100\ \text{Mpc}$, we can rearrange Equation 3 so that it yields the maximum mass of the source of these particles.

$$M = \frac{c^2}{2G}\frac{d}{n} \tag{4}$$

Our ultra high energy proton of 10^{20} eV with $n = 2.27181 \times 10^{22}$ and $d = 100\ \text{Mpc}$ or 3.086 × 10^{26} cm the above equation yields: $0.046M_\odot$ or 48 Jupiter masses. This is the mass of a brown dwarf, whose masses lie in the range 0.013 to $0.075M_\odot$, which is 13 to 75 Jupiter masses [113]-[118].

Brown dwarfs are expected to produce energetic protons through magnetic activity analogous to stellar flares. This is because many brown dwarfs possess the same properties that are listed in the introduction for main sequence stars which lead to solar flare type events [119]-[123].

We turn to investigating the range of brown dwarfs masses that are the sources of ultra high energy cosmic protons. To accomplish this task we rearrange Equation 3 or 4.

$$n = \frac{c^2}{2G}\frac{d}{M} \tag{5}$$

With $d = 100\ \text{Mpc}$ or 3.086 × 10^{26} cm for the maximum mass of a brown dwarf, $0.075M_\odot$, we obtain: $n = 1.39312 \times 10^{22}$ and for the minimum mass of a brown dwarf, $0.013M_\odot$, $n = 8.03724 \times 10^{22}$, whereby n is the distance of the source in Schwarzschild radii, α. Now our task is to convert n into E, the measured proton energy. The most convenient relationship to employ is [13]:

$$n = \frac{m^2 + 2mE + E^2 + \sqrt{2m^3E + 5m^2E^2 + 4mE^3 + E^4}}{m^2} \tag{6}$$

where m is the proton rest mass.

Equation (6) was obtained by solving the relationship between the measured proton energy, E and n: $E = (\gamma - 1)m = \left(\frac{1}{\sqrt{1 - \left(1 - \frac{1}{n}\right)^2}} - 1\right)m$ whereby $\gamma = \frac{1}{\sqrt{1 - v^2}} = \frac{1}{\sqrt{1 - \left(1 - \frac{\alpha}{r}\right)^2}}$ and $v^2 = \left(\frac{\mathrm{d}r}{\mathrm{d}t}\right)^2 = \left(1 - \frac{\alpha}{r}\right)^2$.

Curve fitting Equation (6) leads to:

$$E = 10^{a + b(\log_{10} n)^c} \tag{7}$$

with $a = 8.805645474 \pm 0.000562541$, $b = 0.503052028 \pm 0.000125021$ and $c = 0.998548883 \pm 6.18829 \times 10^{-5}$. Inserting the values of n we derived into this equation we obtain for the maximum mass of a brown dwarf $E = 7.85714 \times 10^{19}\ \text{eV}$ and for the minimum mass of a brown dwarf $E = 1.88741 \times 10^{20}\ \text{eV}$. We conclude that brown dwarfs are the source of ultra high energy cosmic protons in this energy range.

Specifically, brown dwarfs provide a seed population of protons of GeV energy, which is the prerequisite for gravitational repulsion to occur according to Inequality 1. Such protons are then accelerated to very high and ultra high energy via gravitational repulsion.

Brown dwarfs may actually be better proton accelerators than solar-type stars. In order to understand why we need to invoke a simple order of magnitude relationship which yields the maximum particle energy attainable in a magnetized accelerator. It can be estimated from the Hillas confinement condition

$$E_{\max} \sim ZeBL\beta \tag{8}$$

where E is the induced electric field, Z the particle charge, e the elementary charge, B the magnetic field strength, L the size of the acceleration region, and $\beta = v/c$ the reconnection speed in units of c [18]. The key feature of this equation is that the maximum particle energy scales linearly with magnetic field strength. While the magnetic field of the sun in active regions is in the range, 0.1 - 0.3 kG and active M-dwarfs, 1 - 4 kG [124]-[129], the brown dwarf range is: 1 - 5 kG [130] [131]. Thus, brown dwarfs can have magnetic fields an order of magnitude stronger than the Sun. In addition brown dwarfs rotation periods are in the range, 2-10 hours [122] [132]-[136], while the solar value is 25 days. Rapid rotation strengthens the dynamo mechanism, producing stronger magnetospheres and more violent reconnection events. Finally, we note that the observed flare energies from brown dwarfs reach $E_{\text{flare}} \sim 10^{34}$ - 10^{38} erg [123]. These are comparable to or larger than large solar flares. These properties mean that brown dwarfs are expected to produce higher energetic protons than solar-type stars.

We point out that Photo-ionization processes contribute to the ionization of the substellar atmosphere and magnetosphere, thereby increasing the population of free charged particles available for acceleration. However, photo-ionization itself does not accelerate protons to relativistic energies. The production of high-energy seed protons is instead attributed to magnetic processes such as flares, reconnection, and auroral currents, while the subsequent acceleration to very high and ultra high energies is provided by gravitational repulsion in the Schwarzschild field of the source.

Equation (5) shows that if d is smaller the proton energy will be smaller too. So brown dwarfs are also responsible for proton energies < 7.857 × 10^{19} eV. However for protons energies > 1.887 × 10^{20} brown dwarfs are not the source as we make clear in section 3.4.

3.3.1. Energetics Requirement

The observed ultra high energy cosmic ray (UHECR) flux corresponds to a local energy generation rate of approximately

$$\dot{\varepsilon}_{\text{UHECR}} \sim (1 - 5) \times 10^{44}\ \text{erg} \cdot \text{Mpc}^{-3} \cdot \text{yr}^{-1} \tag{9}$$

for particles above ~10^{19} eV [137] [138].

We adopt a fiducial population of 10^{15} for the number of brown dwarfs within 100 Mpc. We obtained this value by using the present-day star-to-brown-dwarf number ratio of approximately 4:1 and the average mass per object derived from the full-sky 20 pc census [139], together with the mean stellar mass density of the Local Volume, $\Omega_\star \simeq 0.0044$ of the critical density [140], one obtains a brown-dwarf number density of order

$$n_{\mathrm{BD}} \sim 3\times10^{8}\ \mathrm{Mpc}^{-3}.$$

Hence the number of brown dwarfs within 100 Mpc is

$$N_{\mathrm{BD}}\left(<100\ \mathrm{Mpc}\right) \simeq \frac{4\pi}{3}\left(100\ \mathrm{Mpc}\right)^{3} n_{\mathrm{BD}} \sim 10^{15}.$$

The time-averaged UHECR power required per brown dwarf is therefore

$$\left\langle \dot{E}_{\mathrm{UHECR}} \right\rangle_{\mathrm{BD}} \approx \left(3\times10^{35} - 2\times10^{36}\right)\mathrm{erg}\cdot\mathrm{yr}^{-1}. \tag{10}$$

If only a fraction, f_{act}, of brown dwarfs is active and each active object produces a UHECR yield E_{evt} every Δt years, then

$$f_{\mathrm{act}}\frac{E_{\mathrm{evt}}}{\Delta t} \approx \left(3\times10^{35} - 2\times10^{36}\right)\mathrm{erg}\cdot\mathrm{yr}^{-1}. \tag{11}$$

Thus the energetics requirement can be satisfied if a few percent of brown dwarfs produce ~10^{37} erg in UHECRs per year-equivalent, or ~10^{38} erg once per decade.

3.3.2. Seed-Particle Acceleration and the Hillas Limit

In convenient units Equation 8 becomes:

$$E_{\max} \simeq 300 Z\beta B[\mathrm{G}]L[\mathrm{c}m]\,\mathrm{eV}. \tag{12}$$

For brown dwarfs with magnetic fields of order 10^3 - 5×10^3 G and characteristic size $L \sim 7\times10^{9}$ cm, which comes from the typical radius of a brown dwarf. Brown dwarfs have radii comparable to Jupiter, typically:

$R_{\mathrm{BD}} \approx 0.7 - 1.4R_J$ with only weak dependence on mass [113] [141]-[146]. Using $R_J = 7.1\times10^{9}\ \mathrm{cm}$, a characteristic size for a brown dwarf is therefore $L \sim 7\times10^{9}\ \mathrm{cm}$.

$$E_{\max}^{(\mathrm{BD})} \sim 10^{15} - 10^{16}\ \mathrm{eV}. \tag{13}$$

Thus magnetospheric activity in substellar objects can plausibly produce relativistic seed particles but does not reach the full UHECR energy range. The Hillas limit therefore determines the seed-particle energy, while the subsequent Schwarzschild gravitational repulsion stage provides the final acceleration to the observed energies above 10^{19} eV.

3.3.3. Source Density and Approximate Isotropy

Another major constraint on UHECR models is the effective source density required to avoid strong clustering in the observed sky. Analyses of UHECR anisotropy typically require source densities exceeding roughly

$$n_{\mathrm{src}} \gtrsim 10^{-4}\ \mathrm{Mpc}^{-3}.$$

[147]-[149] For brown dwarfs the available source density is enormously larger:

$$n_{\mathrm{BD}} \sim 2\times10^{8}\ \mathrm{Mpc}^{-3}. \tag{14}$$

Consequently even an extremely small active fraction yields a very large effective source population. The aggregate emission from such a dense population behaves much more like a quasi-continuous emissivity field than like a sparse set of discrete point sources.

This naturally produces a largely smooth UHECR sky with only weak anisotropy tracing the large-scale matter distribution, broadly consistent with current observations [150]-[153].

3.3.4. Propagation Constraints and the GZK Horizon

UHECR propagation distances are limited by interactions with the cosmic microwave background (CMB). Above ~5 × 10^{19} eV, protons lose energy through photopion production

$$p+\gamma_{\mathrm{CMB}} \to \Delta^{+} \to p\pi^{0} \text{ or } n\pi^{+},$$

which restricts the effective source distance to of order ~100 Mpc [99] [100].

Typical attenuation lengths are

$$D_{\mathrm{att}}(E) \approx \begin{array}{ll} \mathcal{O}(1)\ \mathrm{Gpc} & \text{for } E\sim10^{19}\ \mathrm{eV}, \\ \mathcal{O}(100)\ \mathrm{Mpc} & \text{for } E\sim5\times10^{19}\ \mathrm{eV}, \\ \mathcal{O}(10)-50\ \mathrm{Mpc} & \text{for } E\sim10^{20}\ \mathrm{eV}. \end{array}$$

Thus the observed UHECR flux must originate predominantly from sources inside the local universe within the GZK horizon. Even within a sphere of radius 100 Mpc, however, the expected number of brown dwarfs is of order

$$N_{\mathrm{BD}}(<100\ \mathrm{Mpc}) \sim 10^{15}.$$

Therefore the local universe contains an enormous reservoir of potential seed-particle injectors,

3.3.5. Replacement of the Single Fixed 100 Mpc Horizon

In the above we have assumed that the GZK horizon is a fixed number of 100 Mpc. However, the attenuation length depends on the proton energy. In this section instead of assuming a single fixed propagation horizon, we treat the relevant attenuation length as an energy and composition dependent quantity $D_{\mathrm{att}}(E,A)$ in order to show how the inferred source-mass bounds would change. For proton primaries, the attenuation length is of order Gpc at 10^{18} - 10^{19} eV, decreases to roughly 100 - 200 Mpc near 5 × 10^{19} eV, and falls to only ~10 - 50 Mpc by 10^{20} - $10^{20.5}$ eV due to photopion production on the cosmic microwave background [17] [154] [155]. For heavier nuclei the propagation horizon is also composition dependent because of photodisintegration processes.

Accordingly, any source-mass bound previously written using a fixed 100 Mpc horizon should be interpreted as

$$M_{\text{bound}}(E,A) = M_{\text{bound}}^{(100)}(E)\left[\frac{D_{\text{att}}(E,A)}{100\ \text{Mpc}}\right]^{\delta},$$

where δ is the distance exponent appearing in the underlying derivation. Thus the inferred bounds shift upward at 10^{18} - 10^{19} eV and downward at 10^{20} - $10^{20.5}$ eV relative to the fixed-distance approximation.

3.3.6. Testable Predictions

The brown dwarf seed particle scenario combined with the Schwarzschild gravitational repulsion acceleration stage leads to several observational signatures that can be tested with current ultra high energy cosmic ray datasets.

1) Weak correlation with nearby galaxy catalogs

Because brown dwarfs and planetary-mass objects are ubiquitous constituents of galaxies, the predicted UHECR sky should correlate weakly with the large-scale distribution of nearby galaxies rather than with rare source classes such as powerful AGN or gamma-ray bursts. Cross-correlation analyses using existing galaxy catalogs (e.g., 2MASS, Cosmicflows, or HECATE) therefore provide a direct test of the model.

2) Energy-dependent anisotropy amplitude

As the UHECR energy increases, the propagation horizon decreases due to interactions with the cosmic microwave background. In a model where the effective number of contributing sources inside the horizon is very large, the anisotropy amplitude should scale approximately with the inverse square root of the number of contributing sources,

$$A(E) \propto N^{-1/2} \propto D_{\text{att}}(E)^{-3/2},$$

where $D_{\text{att}}(E)$ is the energy-dependent attenuation length. The model therefore predicts a gradual increase in anisotropy amplitude toward the highest energies.

The acceleration mechanism considered here is spherically symmetric and does not depend on anisotropies in the interior structure of the source or in the cosmological background. Gravitational repulsion in the Schwarzschild field depends only on the mass of the source and the radial motion of the particle. Therefore, anisotropy enters only at the observational level through the spatial distribution of sources and propagation effects, not through the acceleration process itself. This distinguishes the present model from jet-based or shock-acceleration scenarios, in which anisotropic geometries play a central role in particle acceleration.

3) Absence of strong point-source clustering

Because the candidate source population is extremely numerous, the observed UHECR sky should appear as the superposition of many weak sources rather than a few dominant objects. Consequently the model predicts little or no statistically significant point-source clustering even at the highest energies.

4) Characteristic seed-acceleration scale

Magnetospheric processes in substellar objects accelerate charged particles up to a characteristic seed energy determined by the magnetic field strength and size of the object. This scale may imprint a spectral transition separating the seed-acceleration regime from the subsequent gravitational acceleration stage.

Future measurements of the energy spectrum, anisotropy amplitude, and cross-correlations with nearby galaxy catalogs using data from the Pierre Auger Observatory and Telescope Array will therefore provide direct tests of the model.

3.4. The "Oh-My-God" Particle

The highest energy cosmic ray particle ever detected had an energy of 3.2×10^{20} eV. It was detected in 1991 by the Fly's Eye Experiment in Utah [156]. This ultra high energy cosmic ray particle is referred to as the "Oh-My-God" particle. It was most likely a proton, but the possibility of it being a more massive nucleus can not be excluded. Here we assume it was a proton.

Inserting the energy of this particle in Equation 6 leads to: $n = 2.326 \times 10^{23}$, which is more than an order of magnitude beyond the maximum value brown dwarfs can achieve. Inserting this value of n along with $d = 100\ \text{Mpc}$ into Equation 4 we obtain: $M = 0.0045 M_\odot$, which is 4.7 Jupiter masses.

It is thought that such celestial bodies can produce protons in the KeV-MeV range and even up to 100 MeV in extreme conditions [130] [157]. The prerequisite for gravitational repulsion, Inequality 1, however, requires the production of protons in the GeV energy range. Our theory therefore predicts that such a planetary mass body can under extreme conditions produce such proton energies. This circumstance explains why there are so extremely few detections [158], of ultra high energy particles with $E > 1.887 \times 10^{20}\ \text{eV}$.

3.5. Energy Spectrum

The differential ultra high energy cosmic-ray spectrum can be approximated by a broken power law

$$\frac{\mathrm{d}N}{\mathrm{d}E} \propto E^{-\gamma}.$$

Observations show spectral indices of approximately $\gamma \simeq 3.3$ below the ankle and $\gamma \simeq 2.6$ above it. In the present scenario the injected spectrum from the acceleration process is expected to be relatively hard, with an index $\gamma_{inj} \approx 2$, consistent with many astrophysical acceleration mechanisms. Propagation effects during intergalactic transport—primarily pair production and photo pion interactions with the cosmic microwave background—steepen the spectrum and produce the observed indices. The ankle at $E \simeq 5 \times 10^{18}\ \text{eV}$ is interpreted as the transition between the Galactic component and the extragalactic component supplied by substellar seed particle sources. The suppression above ~4×10^{19} eV arises naturally from the GZK energy-loss process together with the maximum attainable energy in the acceleration mechanism. A shallow dip below the ankle can arise from electron–positron pair production by extragalactic protons interacting with the cosmic microwave background [17] [155] [159].

4. Sources of Very High and Ultra High Energy Cosmic Ray Protons

In this section we show how both main sequence stars and brown dwarfs are responsible for the acceleration of cosmic ray protons to very high energy, $10^{15}\ \text{eV} \le E < 10^{18}\ \text{eV}$, and ultra high energy in the range: $E \ge 10^{18}\ \text{eV}$ and $E \le 1.887 \times 10^{20}\ \text{eV}$.

Our conclusion that very high and ultra high energy cosmic ray protons come from sources within the GZK horizon is not new [16] [97] [101] [102] [150] [152] [160]-[162]. The fact that the sources are within the GZK horizon means that our theory resolves the GZK paradox.

4.1. Source Location and Range of Proton Energy Produced by Brown Dwarfs

Figure 1 shows proton energy as a function of the mass of a brown dwarf source. The top red curve assumes the distance of the source is 100 Mpc, the maximum distance a cosmic ray proton can have according to the GZK effect. The radius of the stellar halo of the Milky Way is between 100 and 150 kpc [163]-[167]. Therefore the maximum distance as observed from the sun, which is 8.2 kpc from the galactic center is: between 108 kpc and 158 kpc. In the figure we just use the mean of these two values: 133 kpc. Therefore any brown dwarf proton source between the red and blue curves is extragalactic in origin.

Figure 1 contains four sections. 1) There can be no cosmic ray protons from brown dwarfs above the red line, which is indicated with the word "Forbidden". This is due to the GZK effect. 2) Between the red and blue curves the proton sources are extragalactic brown dwarfs. 3) Between the blue curve and black curve

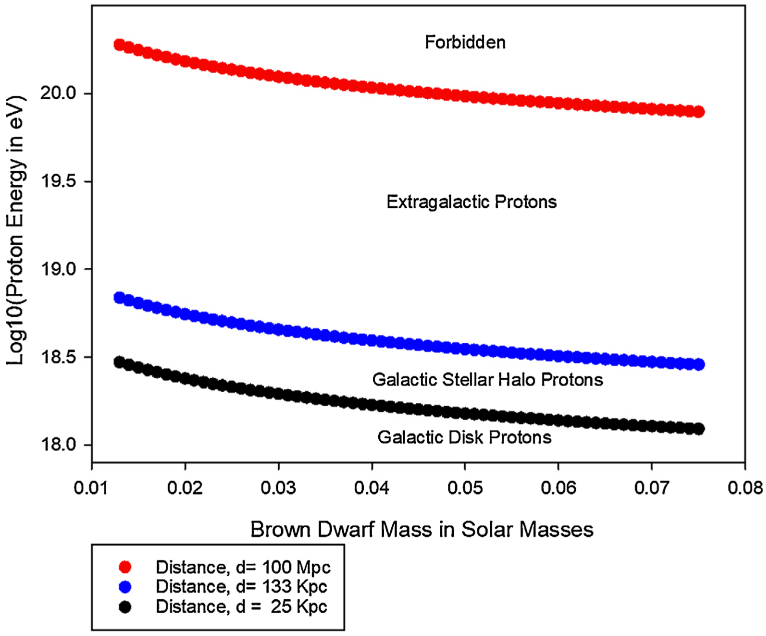

Figure 1. Proton energy as a function of brown dwarf mass.

the proton sources are brown dwarfs located in the galactic halo. 4) Below the black curve the brown dwarf proton sources are located in the disk of the Galaxy.

4.2. Source Location and Range of Proton Energy Produced by Main Sequence Stars

Figure 2 shows the proton energy as a function of stellar mass. The top red curve assumes the distance of the source is 100 Mpc, the maximum distance a cosmic ray proton can have according to the GZK effect. The radius of the stellar halo of the Milky Way is between 100 and 150 kpc. Therefore the maximum distance as observed from the sun, which is 8.2 kpc from the galactic center is: between 108 kpc and 158 kpc. In the figure we just use the mean of these two values: 133 kpc. Therefore any stellar proton source between the red and blue curves is extragalactic in origin.

Figure 2 contains four sections. 1) There can be no cosmic ray protons from stars above the red line, which is indicated with the word "Forbidden". This is due to the GZK effect. 2) Between the red and blue curves the proton sources are extragalactic stars. 3) Between the blue curve and black curve the proton sources are stars located in the galactic halo. 4) Below the black curve the stellar proton sources are located in the disk of the Galaxy.

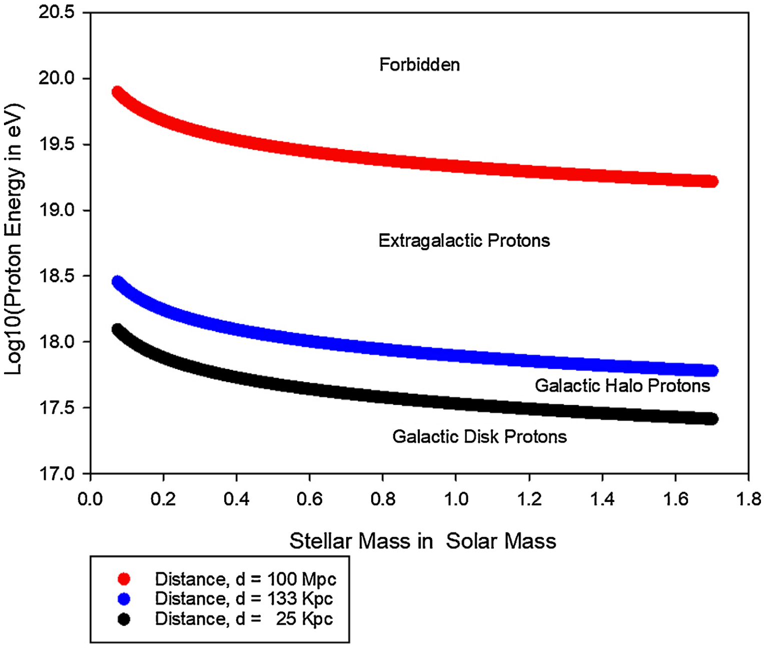

Figure 2. Proton energy as a function of stellar mass.

5. Conclusions

Although shock acceleration in AGN environments is widely proposed as a mechanism for producing very high and ultra high energy cosmic ray protons, current observational evidence has not confirmed this model. In contrast we suggest the acceleration of protons to very high and ultra high energy is not caused by shocks rather by gravitational repulsion in the Schwarzschild field of the source. Our theory makes clear that the sources can not be AGNs rather they are brown dwarfs and main sequence stars whereby in rare ultra high energy events the source posses planetary mass. The fact that the sources are within the GZK horizon means that our theory resolves the GZK paradox.

The meaning of Occam's Razor is: "The more assumptions you have to make, the more unlikely an explanation" (Wikipedia). Our theory requires that protons in radial motion in the Schwarzschild field obey Inequality 1, which means they experience gravitational repulsion. Compare this with the seven assumptions listed in the introduction required for shocks to produce ultra high energy protons. Also compare the mathematics required for shocks as reflected in the publications cited with the simplicity of our mathematics. It is manifest that our theory complies with Occam's Razor.

Many thanks to the family of Dr. and Mrs. William McCormick, whose generous support has provided the prerequisite financial basis and most importantly the necessary time to complete this project.

Conflicts of Interest

The author declares no conflicts of interest regarding the publication of this paper.

References

[1] de la Fuente Marcos, R. and de la Fuente Marcos, C. (2015) On the Angular Distribution of IceCube High-Energy Events. *Astronomische Nachrichten*, **336**, 657-664. https://doi.org/10.1002/asna.201512210

[2] Abbasi, R., Ackermann, M., Adams, J., Agarwalla, S.K., Aguilar, J.A., Ahlers, M., *et al*. (2025) Constraints on the Correlation of IceCube Neutrinos with Tracers of Large-scale Structure. arXiv: 2510.18119.

[3] Guevel, D., Fang, K., (2023) IceCube Collaboration: Cross Correlation of IceCube Neutrinos with Tracers of Large Scale Structure. arXiv: 2308.03978.

[4] Fang, K., Banerjee, A., Charles, E. and Omori, Y. (2020) A Cross-Correlation Study of High-Energy Neutrinos and Tracers of Large-Scale Structure. *The Astrophysical Journal*, **894**, Article 112. https://doi.org/10.3847/1538-4357/ab8561

[5] The IceCube, Auger, P. and Telescope Array Collaborations (2016) Search for Correlations between the Arrival Directions of IceCube Neutrino Events and Ultrahigh-Energy Cosmic Rays Detected by the Pierre Auger Observatory and the Telescope Array. *Journal of Cosmology and Astroparticle Physics*, **2016**, Article 37. https://doi.org/10.1088/1475-7516/2016/01/037

[6] Bellenghi, C., Glauch, T., Haack, C., Kontrimas, T., Niederhausen, H., Reimann, R., Wolf, M. and IceCube Collaboration (2021) A New Search for Neutrino Point Sources with IceCube. arXiv: 2107.08700.

[7] Globus, N. and Blandford, R.D. (2025) Ultrahigh-Energy Cosmic Rays. *Annual Review of Astronomy and Astrophysics*, **63**, 339-377. https://doi.org/10.1146/annurev-astro-052622-033150

[8] Globus, N. and Blandford, R. (2023) Ultra High Energy Cosmic Ray Source Models: Successes, Challenges and General Predictions. *EPJ Web of Conferences*, **283**, Article ID: 04001. https://doi.org/10.1051/epjconf/202328304001

[9] Bister, T. (2025) Probing the Sources of Ultra-High-Energy Cosmic Rays—Constraints from Cosmic-Ray Measurements. *Universe*, **11**, Article 331. https://doi.org/10.3390/universe11100331

[10] Alves Batista, R., Biteau, J., Bustamante, M., Dolag, K., Engel, R., Fang, K., *et al.* (2019) Open Questions in Cosmic-Ray Research at Ultrahigh Energies. *Frontiers in Astronomy and Space Sciences*, **6**, Article 23. https://doi.org/10.3389/fspas.2019.00023

[11] Letessier-Selvon, A. and Stanev, T. (2011) Ultrahigh Energy Cosmic Rays. *Reviews of Modern Physics*, **83**, 907-942. https://doi.org/10.1103/revmodphys.83.907

[12] Uryson, A.V. (2006) Ultra High Energy Cosmic Rays: Identification of Possible Sources, Energy Spectra, and Propagation. *Physics of Particles and Nuclei*, **37**, 347-367. https://doi.org/10.1134/s106377960603004x

[13] McGruder III, C.H. (2026) The Cosmic Origin of High Energy Neutrinos, Ultra High Energy Neutrinos and the Mass of the Muon Neutrino. *Journal of Modern Physics*, **17**, 179-198. https://doi.org/10.4236/jmp.2026.172013

[14] McGruder, C.H. (2017) Acceleration of Particles to High Energy via Gravitational Repulsion in the Schwarzschild Field. *Astroparticle Physics*, **86**, 18-20. https://doi.org/10.1016/j.astropartphys.2016.10.003

[15] Rieger, F.M. (2022) Active Galactic Nuclei as Potential Sources of Ultra-High Energy Cosmic Rays. *Universe*, **8**, Article 607. https://doi.org/10.3390/universe8110607

[16] Kotera, K. and Olinto, A.V. (2011) The Astrophysics of Ultrahigh-Energy Cosmic Rays. *Annual Review of Astronomy and Astrophysics*, **49**, 119-153. https://doi.org/10.1146/annurev-astro-081710-102620

[17] Anchordoqui, L.A. (2019) Ultra-High-Energy Cosmic Rays. *Physics Reports*, **801**, 1-93. https://doi.org/10.1016/j.physrep.2019.01.002

[18] Hillas, A.M. (1984) The Origin of Ultra-High-Energy Cosmic Rays. *Annual Review of Astronomy and Astrophysics*, 22, 425-444. https://doi.org/10.1146/annurev.aa.22.090184.002233

[19] Watson, L.J., Mortlock, D.J. and Jaffe, A.H. (2011) A Bayesian Analysis of the 27 Highest Energy Cosmic Rays Detected by the Pierre Auger Observatory: The Highest Energy Cosmic Rays. *Monthly Notices of the Royal Astronomical Society*, **418**, 206-213. https://doi.org/10.1111/j.1365-2966.2011.19476.x

[20] Terrano, W.A., Zaw, I. and Farrar, G.R. (2012) *CHANDRA* Observations and Classification of Active Galactic Nucleus Candidates Correlated with Auger Uhecrs. *The Astrophysical Journal*, **754**, Article 142. https://doi.org/10.1088/0004-637x/754/2/142

[21] Gureev, S. and Troitsky, S. (2010) Physical Conditions in Nearby Active Galaxies Correlated with Ultra-High-Energy Cosmic Rays Detected by the Pierre Auger Observatory. *International Journal of Modern Physics A*, **25**, 2917-2932. https://doi.org/10.1142/s0217751x10048512

[22] Aloisio, R. and Boncioli, D. (2011) Ultra High Energy Cosmic Rays: Anisotropies and Spectrum. *Astroparticle Physics*, **35**, 152-160. https://doi.org/10.1016/j.astropartphys.2011.05.006

[23] Aab, A., Abreu, P., Aglietta, M., Albuquerque, I.F.M., Allekotte, I., Almela, A., *et al.* (2018) An Indication of Anisotropy in Arrival Directions of Ultra-High-Energy Cosmic Rays through Comparison to the Flux Pattern of Extragalactic Gamma-Ray Sources. *The Astrophysical Journal Letters*, **853**, L29. https://doi.org/10.3847/2041-8213/aaa66d

[24] Abbasi, R.U., Abe, M., Abu-Zayyad, T., Allen, M., Azuma, R., Barcikowski, E., *et al.* (2018) Testing a Reported Correlation between Arrival Directions of Ultra-High-En-

ergy Cosmic Rays and a Flux Pattern from nearby Starburst Galaxies Using Telescope Array Data. *The Astrophysical Journal Letters*, **867**, L27.

[25] Anchordoqui, L.A. (2018) Acceleration of Ultrahigh-Energy Cosmic Rays in Starburst Superwinds. *Physical Review D*, **97**, Article ID: 063010. https://doi.org/10.1103/physrevd.97.063010

[26] Abdul Halim, A., Abreu, P., Aglietta, M., Allekotte, I., Almeida Cheminant, K., Almela, A., *et al.* (2024) Constraining Models for the Origin of Ultra-High-Energy Cos-Mic Rays with a Novel Combined Analysis of Arrival Directions, Spectrum, and Composition Data Measured at the Pierre Auger Observatory. *Journal of Cosmology and Astroparticle Physics*, **2024**, Article 22.

[27] Doghmane, R. and Attallah, R. (2022) Probing Cosmic-Ray Anisotropy at Ultra-High Energy. *Journal of Astrophysics and Astronomy*, **43**, Article No. 89. https://doi.org/10.1007/s12036-022-09887-8

[28] Vietri, M., De Marco, D. and Guetta, D. (2003) On the Generation of Ultra-High-Energy Cosmic Rays in γ-Ray Bursts: A Reappraisal. *The Astrophysical Journal*, **592**, 378-389. https://doi.org/10.1086/375719

[29] Dermer, C.D., McEnery, J.E., Racusin, J.L. and Gehrels, N. (2011) Are γ-Ray Bursts the Sources of the Ultra-High Energy Cosmic Rays? *AIP Conference Proceedings*, **1358**, 355-360. https://doi.org/10.1063/1.3621804

[30] Baerwald, P., Bustamante, M. and Winter, W. (2015) Are γ-Ray Bursts the Sources of Ultra-High Energy Cosmic Rays? *Astroparticle Physics*, **62**, 66-91. https://doi.org/10.1016/j.astropartphys.2014.07.007

[31] Zhang, B.T., Murase, K., Kimura, S.S., Horiuchi, S. and Mészáros, P. (2018) Low-luminosity γ-Ray Bursts as the Sources of Ultrahigh-Energy Cosmic Ray Nuclei. *Physical Review D*, **97**, Article ID: 083010. https://doi.org/10.1103/physrevd.97.083010

[32] Wang, X., Razzaque, S. and Mészáros, P. (2008) On the Origin and Survival of Ultra-High-Energy Cosmic-Ray Nuclei in γ-Ray Bursts and Hypernovae. *The Astrophysical Journal*, **677**, 432-440. https://doi.org/10.1086/529018

[33] He, H., Zhang, B.T. and Fan, Y. (2024) A Detectable Ultra-High-Energy Cosmic-Ray Outburst from GRB 221009A. *The Astrophysical Journal*, **963**, Article 109. https://doi.org/10.3847/1538-4357/ad2352

[34] Ryu, D., Kang, H., Hallman, E. and Jones, T.W. (2003) Cosmological Shock Waves and Their Role in the Large-Scale Structure of the Universe. *The Astrophysical Journal*, **593**, 599-610. https://doi.org/10.1086/376723

[35] Norman, C.A., Melrose, D.B. and Achterberg, A. (1995) The Origin of Cosmic Rays above 10 18.5 eV. *The Astrophysical Journal*, **454**, 60. https://doi.org/10.1086/176465

[36] Kang, H. and Ryu, D. (2013) Diffusive Shock Acceleration at Cosmological Shock Waves. *The Astrophysical Journal*, **764**, Article 95. https://doi.org/10.1088/0004-637x/764/1/95

[37] Gabici, S. (2003) γ-Ray Emission from Clusters of Galaxies. arXiv: astro-ph/0307499.

[38] Vazza, F., Brunetti, G. and Gheller, C. (2009) Shock Waves in Eulerian Cosmological Simulations: Main Properties and Acceleration of Cosmic Rays. *Monthly Notices of the Royal Astronomical Society*, **395**, 1333-1354. https://doi.org/10.1111/j.1365-2966.2009.14691.x

[39] Blasi, P. (2013) The Origin of Galactic Cosmic Rays. *The Astronomy and Astrophysics Review*, **21**, Article No. 70. https://doi.org/10.1007/s00159-013-0070-7

[40] Blasi, P., Epstein, R.I. and Olinto, A.V. (2000) Ultra-High-Energy Cosmic Rays from

Young Neutron Star Winds. *The Astrophysical Journal*, **533**, L123-L126. https://doi.org/10.1086/312626

[41] Arons, J. (2003) Magnetars in the Metagalaxy: An Origin for Ultra-High-Energy Cosmic Rays in the Nearby Universe. *The Astrophysical Journal*, **589**, 871-892. https://doi.org/10.1086/374776

[42] Kotera, K. and Amato, E. (2015) Engines of Radio Transients: Neutron Star Birth and Cosmic Rays. *Annual Review of Nuclear and Particle Science*, **65**, 449-472.

[43] Fang, K., Kotera, K. and Olinto, A.V. (2014) Newly Born Pulsars as Sources of Ultra-high Energy Cosmic Rays. arXiv: 1201.5197.

[44] Fang, K. and Olinto, A.V. (2016) High-Energy Neutrinos from Sources in Clusters of Galaxies. *The Astrophysical Journal*, **828**, 37. https://doi.org/10.3847/0004-637X/828/1/37

[45] Murase, K., Kashiyama, K. and Mészáros, P. (2014) A New Class of High-Energy Transients from Crustal Failure of Neutron Stars during Binary Mergers. *Monthly Notices of the Royal Astronomical Society*, **442**, 60-64.

[46] Farrar, G.R. (2025) Binary Neutron Star Mergers as the Source of the Highest Energy Cosmic Rays. *Physical Review Letters*, **134**, Article ID: 081003. https://doi.org/10.1103/physrevlett.134.081003

[47] Rodrigues, X., Biehl, D., Boncioli, D. and Taylor, A.M. (2019) Binary Neutron Star Merger Remnants as Sources of Cosmic Rays Below the "Ankle". *Astroparticle Physics*, **106**, 10-17. https://doi.org/10.1016/j.astropartphys.2018.10.007

[48] Guo, G., Qian, Y. and Wu, M. (2025) Binary Neutron Star Mergers as Potential Sources for Ultrahigh-Energy Cosmic Rays and High-Energy Neutrinos. *Physical Review D*, **112**, Article ID: 063022. https://doi.org/10.1103/zfp3-y9yw

[49] Zhang, B.T., Murase, K., Oikonomou, F. and Li, Z. (2017) High-Energy Cosmic Ray Nuclei from Tidal Disruption Events: Origin, Survival, and Implications. *Physical Review D*, **96**, Article ID: 063007. https://doi.org/10.1103/physrevd.96.063007

[50] Biehl, D., Boncioli, D., Lunardini, C. and Winter, W. (2018) Tidally Disrupted Stars as a Possible Origin of Both Cosmic Rays and Neutrinos at the Highest Energies. *Scientific Reports*, **8**, Article No. 10828. https://doi.org/10.1038/s41598-018-29022-4

[51] Pfeffer, D.N., Kovetz, E.D. and Kamionkowski, M. (2016) Ultrahigh-Energy Cosmic Ray Hotspots from Tidal Disruption Events. *Monthly Notices of the Royal Astronomical Society*, **466**, 2922-2926. https://doi.org/10.1093/mnras/stw3337

[52] Guépin, C., Kotera, K., Barausse, E., Fang, K. and Murase, K. (2018) Ultra-High-Energy Cosmic Rays and Neutrinos from Tidal Disruptions by Massive Black Holes. *Astronomy & Astrophysics*, **616**, A179. https://doi.org/10.1051/0004-6361/201732392

[53] Reames, D.V. (1999) Particle Acceleration at the Sun and in the Heliosphere. *Space Science Reviews*, **90**, 413-491. https://doi.org/10.1023/a:1005105831781

[54] Giacalone, J. and Kóta, J. (2006) Acceleration of Solar-Energetic Particles by Shocks. *Space Science Reviews*, **124**, 277-288. https://doi.org/10.1007/s11214-006-9110-1

[55] Lee, M.A., Mewaldt, R.A. and Giacalone, J. (2012) Shock Acceleration of Ions in the Heliosphere. *Space Science Reviews*, **173**, 247-281. https://doi.org/10.1007/s11214-012-9932-y

[56] Desai, M. and Giacalone, J. (2016) Large Gradual Solar Energetic Particle Events. *Living Reviews in Solar Physics*, **13**, Article No. 3. https://doi.org/10.1007/s41116-016-0002-5

[57] Li, G., Zank, G.P. and Rice, W.K.M. (2003) Energetic Particle Acceleration and Transport at Coronal Mass Ejection-Driven Shocks. *Journal of Geophysical Research: Space Physics*, **108**, Article 1082. https://doi.org/10.1029/2002ja009666

[58] Afanasiev, A., Vainio, R., Rouillard, A.P., Battarbee, M., Aran, A. and Zucca, P. (2018) Modelling of Proton Acceleration in Application to a Ground Level Enhancement. *Astronomy & Astrophysics*, **614**, A4. https://doi.org/10.1051/0004-6361/201731343

[59] Gopalswamy, N., Xie, H., Yashiro, S., Akiyama, S., Mäkelä, P. and Usoskin, I.G. (2010) Ground Level Enhancement Events of Solar Cycle 23. *International Journal of Remote Sensing and Space Physics*, **39**, 240-248.

[60] Krymskii, G.F. (1977) A Regular Mechanism for the Acceleration of Charged Particles on the Front of a Shock Wave. *Akademiia Nauk SSSR Doklady*, **234**, 1306-1308.

[61] Bell, A.R. (1978) The Acceleration of Cosmic Rays in Shock Fronts—I. *Monthly Notices of the Royal Astronomical Society*, **182**, 147-156. https://doi.org/10.1093/mnras/182.2.147

[62] Bell, A.R. (1978) The Acceleration of Cosmic Rays in Shock Fronts—II. *Monthly Notices of the Royal Astronomical Society*, **182**, 443-455. https://doi.org/10.1093/mnras/182.3.443

[63] Drury, L.O. (1983) An Introduction to the Theory of Diffusive Shock Acceleration of Energetic Particles in Tenuous Plasmas. *Reports on Progress in Physics*, **46**, 973-1027. https://doi.org/10.1088/0034-4885/46/8/002

[64] Blandford, R. and Eichler, D. (1987) Particle Acceleration at Astrophysical Shocks: A Theory of Cosmic Ray Origin. *Physics Reports*, **154**, 1-75. https://doi.org/10.1016/0370-1573(87)90134-7

[65] Baring, M.G. (2004) Diffusive Shock Acceleration of High Energy Cosmic Rays. *Nuclear Physics B—Proceedings Supplements*, **136**, 198-207. https://doi.org/10.1016/j.nuclphysbps.2004.10.008

[66] Peretti, E., Lamastra, A., Saturni, F.G., Ahlers, M., Blasi, P., Morlino, G., *et al.* (2023) Diffusive Shock Acceleration at EeV and Associated Multimessenger Flux from Ultra-Fast Outflows Driven by Active Galactic Nuclei. *Monthly Notices of the Royal Astronomical Society*, **526**, 181-192. https://doi.org/10.1093/mnras/stad2740

[67] Longair, M.S. (2011) Cosmic Ray Astrophysics. Cambridge University Press.

[68] Berezinsky, V.S., Bulanov, S.V., Dogiel, V.A. and Ginzburg, V.L. (1990) Astrophysics of Cosmic Rays. North-Holland Publisher.

[69] Droste, J. (1915) On the Field of a Single Centre in Einstein's Theory of Gravitation. *Koninklijke Nederlandse Akademie van Wetenschappen Proceedings Series B Physical Sciences*, **17**, 998-1011.

[70] Droste, J. (1916) Het zwaartekrachtsveld van een of meer lichamen volgens de theorie van Einstein. Ph.D. Thesis, Leiden University.

[71] Hilbert, D. (1915) Die Grundlagen der Physik. (Erste Mitteilung). *Nachrichten von der Königlichen Gesellschaft der Wissenschaften zu Göttingen, Mathematisch-Physikalische Klasse*, 395-407.

[72] Hilbert, D. (1916) Die Feldgleichungen der Gravitation. *Nachrichten von der Gesellschaft der Wissenschaften zu Göttingen, Mathematisch-Physikalische Klasse*, **48**, 844-847.

[73] Hilbert, D. (1917) Die Grundlagen der Physik (Zweite Mitteilung). *Nachrichten von der Gesellschaft der Wissenschaften zu Göttingen, Mathematisch-Physikalische Klasse*, 53-76.

[74] McGruder III, C.H. and Van Der Meer, B.W. (2018) The 1916 PhD Thesis of Johannes Droste and the Discovery of Gravitational Repulsion. arXiv: 1801.07592.

[75] McGruder, C.H. (1982) Gravitational Repulsion in the Schwarzschild Field. *Physical Review D*, **25**, 3191-3194. https://doi.org/10.1103/physrevd.25.3191

[76] Aiello, S., Albert, A., Alhebsi, A.R., Alshamsi, M., Alves Garre, S., Ambrosone, A., *et al.* (2025) Observation of an Ultra-High-Energy Cosmic Neutrino with KM3NeT. *Nature*, **638**, 376-382. https://doi.org/10.1038/s41586-024-08543-1

[77] Krori, K.D., Sarmah, J.C. and Goswami, D. (1984) Gravitational Repulsion in the Einstein-Zero-Mass Scalar Theory. *Canadian Journal of Physics*, **62**, 629-631. https://doi.org/10.1139/p84-085

[78] P L Bragança, D. (2024) Gravitational Repulsion in an Expanding Ball of Dust. *Classical and Quantum Gravity*, **41**, Article ID: 075008. https://doi.org/10.1088/1361-6382/ad2d70

[79] Polo, C.L. and Singh, H.S. (2024) Hilbert Repulsion in the Kerr-Newman Anti-De Sitter Spacetime. *Astrophysics and Space Science*, **369**, Article No. 41. https://doi.org/10.1007/s10509-024-04304-8

[80] Célérier, M.N., Santos, N.O. and Satheeshkumar, V.H. (2017) Hilbert Repulsion in the Reissner-Nordström and Schwarzschild spacetimes. arXiv: 1707.06994.

[81] Gorkavyi, N. and Vasilkov, A. (2016) A Repulsive Force in the Einstein Theory. *Monthly Notices of the Royal Astronomical Society*, **461**, 2929-2933. https://doi.org/10.1093/mnras/stw1517

[82] Kutschera, M. and Zajiczek, W. (2009) Shapiro Effect for for Relativistic Particles-Testing General Relativity in a New Window. arXiv: 0906.5088.

[83] Herrera, L. (2005) Geodesics in a Quash-Spherical Spacetime: A Case of Gravitational Repulsion. *Foundations of Physics Letters*, **18**, 21-36. https://doi.org/10.1007/s10702-005-2467-7

[84] Ponce de Leon, J. (1988) Gravitational Repulsion in Sources of the Reissner-Nordström Field. *Journal of Mathematical Physics*, **29**, 197-206. https://doi.org/10.1063/1.528172

[85] Krori, K.D. and Barua, M. (1985) Gravitational Repulsion by Kerr and Kerr-Newman Black Holes. *Physical Review D*, **31**, 3135-3139. https://doi.org/10.1103/physrevd.31.3135

[86] Greene, J.E. and Ho, L.C. (2007) The Mass Function of Active Black Holes in the Local Universe. *The Astrophysical Journal*, **667**, 131-148.

[87] Blandford, R.D. and McKee, C.F. (1982) Reverberation Mapping of the Emission Line Regions of Seyfert Galaxies and Quasars. *The Astrophysical Journal*, **255**, 419-439. https://doi.org/10.1086/159843

[88] Peterson, B.M., Ferrarese, L., Gilbert, K.M., Kaspi, S., Malkan, M.A., Maoz, D., *et al.* (2004) Central Masses and Broad-line Region Sizes of Active Galactic Nuclei. II. A Homogeneous Analysis of a Large Reverberation-mapping Database. *The Astrophysical Journal*, **613**, 682-699. https://doi.org/10.1086/423269

[89] Bentz, M.C. and Katz, S. (2015) The AGN Black Hole Mass Database. *Publications of the Astronomical Society of the Pacific*, **127**, 67-73. https://doi.org/10.1086/679601

[90] Vestergaard, M. and Peterson, B.M. (2006) Determining Central Black Hole Masses in Distant Active Galaxies and Quasars. II. Improved Optical and UV Scaling Relationships. *The Astrophysical Journal*, **641**, 689-709. https://doi.org/10.1086/500572

[91] Shen, Y., Richards, G.T., Strauss, M.A., Hall, P.B., Schneider, D.P., Snedden, S., *et al.* (2011) A Catalog of Quasar Properties from Sloan Digital Sky Survey Data Release 7. *The Astrophysical Journal Supplement Series*, **194**, Article 45. https://doi.org/10.1088/0067-0049/194/2/45

[92] Shen, Y., Strauss, M.A., Oguri, M., Hennawi, J.F., Fan, X., Richards, G.T., *et al.* (2007) Clustering of High-Redshift ($z \geq 2.9$) Quasars from the Sloan Digital Sky Survey. *The Astronomical Journal*, **133**, 2222-2241. https://doi.org/10.1086/513517

[93] McConnell, N.J., Ma, C., Gebhardt, K., Wright, S.A., Murphy, J.D., Lauer, T.R., *et al.* (2011) Two Ten-Billion-Solar-Mass Black Holes at the Centres of Giant Elliptical Galaxies. *Nature*, **480**, 215-218. https://doi.org/10.1038/nature10636

[94] van den Bosch, R.C.E., Gebhardt, K., Gültekin, K., van de Ven, G., van der Wel, A. and Walsh, J.L. (2012) An Over-Massive Black Hole in the Compact Lenticular Galaxy NGC 1277. *Nature*, **491**, 729-731. https://doi.org/10.1038/nature11592

[95] McConnell, N.J. and Ma, C. (2013) Revisiting the Scaling Relations of Black Hole Masses and Host Galaxy Properties. *The Astrophysical Journal*, **764**, Article 184. https://doi.org/10.1088/0004-637x/764/2/184

[96] Kormendy, J. and Ho, L.C. (2013) Coevolution (or Not) of Supermassive Black Holes and Host Galaxies. *Annual Review of Astronomy and Astrophysics*, **51**, 511-653. https://doi.org/10.1146/annurev-astro-082708-101811

[97] Kachelriess, M. and Serpico, P.D. (2007) The GZK Horizon of Ultra-High Energy Cosmic Rays. arXiv: 0711.3635.

[98] Berezinsky, V., Gazizov, A. and Grigorieva, S. (2006) On Astrophysical Solution to Ultrahigh Energy Cosmic Rays. *Physical Review D*, **74**, Article ID: 043005. https://doi.org/10.1103/physrevd.74.043005

[99] Greisen, K. (1966) End to the Cosmic-Ray Spectrum? *Physical Review Letters*, **16**, 748-750. https://doi.org/10.1103/physrevlett.16.748

[100] Zatsepin, G.T. AND Kuzmin, V.A. (1966) Upper Limit of the Spectrum of Cosmic Rays. *JETP Letters*, **4**, 78-80.

[101] Abbasi, R.U., Abu-Zayyad, T., Allen, M., *et al.* (2008) First Observation of the Greisen-Zatsepin-Kuzmin Suppression. *Physical Review Letters*, **100**, Article ID: 101101.

[102] Abraham, J., Abreu, P., Aglietta, M., *et al.* (2008) Observation of the Suppression of the Flux of Cosmic Rays above 4 1019 ev. *Physical Review Letters*, **101**, Article ID: 061101.

[103] Watson, A.A. (2014) High-Energy Cosmic Rays and the Greisen-Zatsepin-Kuz'min Effect. *Reports on Progress in Physics*, **77**, Article ID: 036901. https://doi.org/10.1088/0034-4885/77/3/036901

[104] Kowalski, A.F. (2024) Stellar Flares. *Living Reviews in Solar Physics*, **21**, Article No. 1. https://doi.org/10.1007/s41116-024-00039-4

[105] Segura, A., Walkowicz, L.M., Meadows, V., Kasting, J. and Hawley, S. (2010) The Effect of a Strong Stellar Flare on the Atmospheric Chemistry of an Earth-Like Planet Orbiting an M Dwarf. *Astrobiology*, **10**, 751-771. https://doi.org/10.1089/ast.2009.0376

[106] Althukair, A. and Tsiklauri, D. (2022) Statistical Properties of Stellar Superflares from f- to m-Type Stars Observed by Kepler. *Astrophysical Journal*, **926**, Article 196.

[107] Bai, T. (1989) Particle Acceleration in Solar Flares. *Annual Review of Astronomy and Astrophysics*, **27**, 421-474.

[108] Burrows, A., Marley, M., Hubbard, W.B., Lunine, J.I., Guillot, T., Saumon, D., *et al.*

(1997) A Nongray Theory of Extrasolar Giant Planets and Brown Dwarfs. *The Astrophysical Journal*, **491**, 856-875. https://doi.org/10.1086/305002

[109] Chabrier, G. and Baraffe, I. (1997) Structure and Evolution of Low-Mass Stars. *Astronomy & Astrophysics*, **327**, 1039-1053.

[110] Baraffe, I., Chabrier, G., Allard, F. and Hauschildt, P.H. (1998) Evolutionary Models for Solar Metallicity Low-Mass Stars: Mass-Magnitude Relationships and Color-Magnitude Diagrams. *Astronomy & Astrophysics*, **337**, 403-412.

[111] Kippenhahn, R., Weigert, A. and Weiss, A. (2012) Stellar Structure and Evolution. 2nd Edition, Springer.

[112] Cox, A.N. (2000) Allen's Astrophysical Quantities. Springer.

[113] Burrows, A., Hubbard, W.B., Lunine, J.I. and Liebert, J. (2001) The Theory of Brown Dwarfs and Extrasolar Giant Planets. *Reviews of Modern Physics*, **73**, 719-765. https://doi.org/10.1103/revmodphys.73.719

[114] Chabrier, G., Phillips, M.W., Baraffe, I., Borysow, A. and Jørgensen, U.G. (2023) New Determination of the Hydrogen Burning Limit. *Astronomy & Astrophysics*, **671**, Article No. A119.

[115] Spiegel, D.S., Burrows, A. and Milsom, J.A. (2011) The Deuterium-Burning Mass Limit for Brown Dwarfs and Giant Planets. *The Astrophysical Journal*, **727**, Article 57. https://doi.org/10.1088/0004-637x/727/1/57

[116] Zuckerman, B. (2000) Brown Dwarfs: At Last Filling the Gap between Stars and Planets. *Proceedings of the National Academy of Sciences of the United States of America*, **97**, 963-966. https://doi.org/10.1073/pnas.97.3.963

[117] Liu, B., Lambrechts, M., Johansen, A., Pascucci, I. and Henning, T. (2020) Pebble-driven Planet Formation around Very Low-Mass Stars and Brown Dwarfs. *Astronomy & Astrophysics*, **638**, A88. https://doi.org/10.1051/0004-6361/202037720

[118] Basri, G. and Brown, M.E. (2006) Planetesimals to Brown Dwarfs: What Is a Planet? *Annual Review of Earth and Planetary Sciences*, **34**, 193-216. https://doi.org/10.1146/annurev.earth.34.031405.125058

[119] Berger, E., Ball, S., Becker, K.M., Clarke, M., Frail, D.A., Fukuda, T.A., *et al.* (2001) Discovery of Radio Emission from the Brown Dwarf LP944-20. *Nature*, **410**, 338-340. https://doi.org/10.1038/35066514

[120] Rodríguez-Barrera, M.I., Helling, C. and Wood, K. (2018) Environmental Effects on the Ionisation of Brown Dwarf Atmospheres. *Astronomy & Astrophysics*, **618**, A107. https://doi.org/10.1051/0004-6361/201832685

[121] Saur, J., Willmes, C., Fischer, C., *et al.* (2021) Brown Dwarfs as Candidates for Detecting UV Aurora Outside the Solar System: Hubble Space Telescope Observations of 2MASS J1237+6526. Astronomy & Astrophysics, 655, Article ID: A75.

[122] Hallinan, G., Littlefair, S.P., Cotter, G., Bourke, S., Harding, L.K., Pineda, J.S., *et al.* (2015) Magnetospherically Driven Optical and Radio Aurorae at the End of the Stellar Main Sequence. *Nature*, **523**, 568-571. https://doi.org/10.1038/nature14619

[123] Gizis, J.E., *et al.* (2017) The White Light Flare Rate of Young Brown Dwarfs. arXiv: 1703.08745.

[124] Reiners, A. and Basri, G. (2007) The First Direct Measurements of Surface Magnetic Fields on Very Low Mass Stars. *The Astrophysical Journal*, **656**, 1121-1135. https://doi.org/10.1086/510304

[125] Reiners, A. and Basri, G. (2009) On the Magnetic Topology of Partially and Fully Convective Stars. *Astronomy & Astrophysics*, **496**, 787-790.

https://doi.org/10.1051/0004-6361:200811450

[126] Johns-Krull, C.M. and Valenti, J.A. (1996) Detection of Strong Magnetic Fields on M Dwarfs. *The Astrophysical Journal*, **459**, L95. https://doi.org/10.1086/309954

[127] Saar, S.H. (1996) Recent Measurements of Stellar Magnetic Fields. *Symposium—International Astronomical Union*, **176**, 237-244. https://doi.org/10.1017/s0074180900083261

[128] Donati, J., Morin, J., Petit, P., Delfosse, X., Forveille, T., Aurière, M., *et al.* (2008) Large-Scale Magnetic Topologies of Early M Dwarfs. *Monthly Notices of the Royal Astronomical Society*, **390**, 545-560. https://doi.org/10.1111/j.1365-2966.2008.13799.x

[129] Shulyak, D., Reiners, A., Engeln, A., *et al.* (2017) Strong Dipole Magnetic Fields in Fast Rotating Fully Convective Stars. *Nature Astronomy*, **1**, Article 184.

[130] Reiners, A. and Christensen, U.R. (2010) A Magnetic Field Evolution Scenario for Brown Dwarfs and Giant Planets. *Astronomy & Astrophysics*, **522**, A13. https://doi.org/10.1051/0004-6361/201014251

[131] Berdyugina, S.V., Harrington, D.M., Kuzmychov, O., Kuhn, J.R., Hallinan, G., Kowalski, A.F., *et al.* (2017) First Detection of a Strong Magnetic Field on a Bursty Brown Dwarf: Puzzle Solved. *The Astrophysical Journal*, **847**, Article 61. https://doi.org/10.3847/1538-4357/aa866b

[132] Bailer-Jones, C.A.L. and Mundt, R. (2001) Variability in Ultra Cool Dwarfs: Evidence for the Evolution of Surface Features. *Astronomy & Astrophysics*, **367**, 218-235. https://doi.org/10.1051/0004-6361:20000416

[133] Mohanty, S. and Basri, G. (2003) Rotation & Activity in Mid-M to L Dwarfs. *The Astrophysical Journal*, **583**, 451-472.

[134] Reiners, A. and Basri, G. (2008) Chromospheric Activity, Rotation, and Rotational Braking in M and L Dwarfs. *The Astrophysical Journal*, **684**, 1390-1403. https://doi.org/10.1086/590073

[135] Metchev, S.A., Heinze, A., Apai, D., Flateau, D., Radigan, J., Burgasser, A., *et al.* (2015) Weather on Other Worlds. II. Survey Results: Spots Are Ubiquitous on L and T Dwarfs. *The Astrophysical Journal*, **799**, Article 154. https://doi.org/10.1088/0004-637x/799/2/154

[136] Zapatero Osorio, M.R., Martin, E.L., Bouy, H., Tata, R., Deshpande, R. and Wainscoat, R.J. (2006) Spectroscopic Rotational Velocities of Brown Dwarfs. *The Astrophysical Journal*, **647**, 1405-1412. https://doi.org/10.1086/505484

[137] Waxman, E. (1995) Cosmological Gamma-Ray Bursts and the Highest Energy Cosmic Rays. *Physical Review Letters*, **75**, 386-389. https://doi.org/10.1103/physrevlett.75.386

[138] Ahlers, M. and Anchordoqui, L.A. (2012) High-Energy Cosmic Rays from Astrophysical Sources: An Overview. *Physical Review D*, **85**, Article ID: 063010.

[139] Kirkpatrick, J.D., Marocco, F., Gelino, C.R., Raghu, Y., Faherty, J.K., Bardalez Gagliuffi, D.C., *et al.* (2024) The Backyard Worlds: Planet 9 Collaboration: The Initial Mass Function Based on the Full-Sky 20 pc Census of 3600 Stars and Brown Dwarfs. arXiv: 2312.03639.

[140] Karachentsev, I.D. and Telikova, K.N. (2018) Stellar and Dark Matter Density in the Local Universe. *Astronomische Nachrichten*, **339**, 615-622. https://doi.org/10.1002/asna.201813520

[141] Luhman, K.L. (2012) The Formation and Early Evolution of Low-Mass Stars and

Brown Dwarfs. *Annual Review of Astronomy and Astrophysics*, **50**, 65-106. https://doi.org/10.1146/annurev-astro-081811-125528

[142] Sorahana, S., Yamamura, I. and Murakami, H. (2013) On the Radii of Brown Dwarfs Measured with *Akari* Near-Infrared Spectroscopy. *The Astrophysical Journal*, **767**, Article 77. https://doi.org/10.1088/0004-637x/767/1/77

[143] Carmichael, T.W. (2022) Improved Radius Determinations for the Transiting Brown Dwarf Population in the Era of *GAIA* and *TESS*. *Monthly Notices of the Royal Astronomical Society*, **519**, 5177-5190. https://doi.org/10.1093/mnras/stac3720

[144] Chabrier, G. and Baraffe, I. (2000) Theory of Low-Mass Stars and Substellar Objects. *Annual Review of Astronomy and Astrophysics*, **38**, 337-377. https://doi.org/10.1146/annurev.astro.38.1.337

[145] Baraffe, I., Chabrier, G., Allard, F. and Hauschildt, P. (2003) Evolutionary Models for Low Mass Stars and Brown Dwarfs at Young Ages. *Symposium—International Astronomical Union*, **211**, 41-50. https://doi.org/10.1017/s0074180900210243

[146] Zapolsky, H.S. and Salpeter, E.E. (1969) The Mass-Radius Relation for Cold Spheres of Low Mass. *The Astrophysical Journal*, **158**, 809. https://doi.org/10.1086/150240

[147] Blasi, P. and De Marco, D. (2004) The Small Scale Anisotropies, the Spectrum and the Sources of Ultra-High Energy Cosmic Rays. *Astroparticle Physics*, **20**, 559-577. https://doi.org/10.1016/j.astropartphys.2003.07.002

[148] Takami, H., Nishimichi, T., Yahata, K. and Sato, K. (2009) Cross-Correlation between UHECR Arrival Distribution and Large-Scale Structure. *Journal of Cosmology and Astroparticle Physics*, **2009**, Article 31. https://doi.org/10.1088/1475-7516/2009/06/031

[149] Pierre Auger Collaboration, Abreu, P., Aglietta, M., Ahlers, M., Ahn, E.J., Albuquerque, I.F.M., Allard, D., *et al.* (2013) Constraints on the Origin of Cosmic Rays above 10^{18} eV from Large-Scale Anisotropy Searches in Data of the Pierre Auger Observatory. *The Astrophysical Journal Letters*, **762**, L13.

[150] Aab, A., Abreu, P., Aglietta, M., *et al.* (2017) Observation of a Large-Scale Anisotropy in the Arrival Directions of Cosmic Rays above 8 Times 10^{18} eV. *Science*, **357**, 1266-1270.

[151] Aab, A., *et al.* (2020) Large-Scale Cosmic-Ray Anisotropies above 4 EeV Measured by the Pierre Auger Observatory. arXiv: 1808.03579.

[152] Abbasi, R.U., Abe, M., Abu-Zayyad, T., Allen, M., Anderson, R., Azuma, R., *et al.* (2014) Indications of Intermediate-Scale Anisotropy of Cosmic Rays with Energy Greater Than 57 EeV in the Northern Sky Measured with the Surface Detector of the Telescope Array Experiment. arXiv: 1404.5890.

[153] Collaboration, P.A. and Collaboration, T.A. (2014) Full-Sky Search for Large-Scale Anisotropies in the Arrival Directions of Cosmic Rays Detected Above 1019 eV. *The Astrophysical Journal*, **794**, 172.

[154] Allard, D. (2012) Extragalactic Propagation of Ultrahigh Energy Cosmic-Rays. *Astroparticle Physics*, **39**, 33-43. https://doi.org/10.1016/j.astropartphys.2011.10.011

[155] Aloisio, R., Berezinsky, V. and Blasi, P. (2017) Ultra-High Energy Cosmic Rays: Implications of Auger Data for Source Spectra and Chemical Composition. *Journal of Cosmology and Astroparticle Physics*, **2017**, Article 20.

[156] Bird, D.J., Corbato, S.C., Dai, H.Y., Elbert, J.W., Green, K.D., Huang, M.A., *et al.* (1995) Detection of a Cosmic Ray with Measured Energy Well Beyond the Expected Spectral Cutoff Due to Cosmic Microwave Radiation. *The Astrophysical Journal*, **441**, 144. https://doi.org/10.1086/175344

[157] Bagheri, F., Lopez, R.E. and Shahmoradi, A. (2024) Infrared-Radio-Follow-Up Observations for Detection of the Magnetic Radio Emission of Extra Solar Planets: A New Window to Detect Exoplanets. *Frontiers in Astronomy and Space Sciences*, **11**, Article 1400032. https://doi.org/10.3389/fspas.2024.1400032

[158] Ohsawa, Y. (2014) Ultrarelativistic Particle Acceleration in Collisionless Shock Waves. *Physics Reports*, **536**, 147-254. https://doi.org/10.1016/j.physrep.2013.11.004

[159] Aab, A., Abreu, P., Aglietta, M., Albury, J.M., Allekotte, I., Almela, A., *et al.* (2020) Features of the Energy Spectrum of Cosmic Rays above 2.5 $\times 10^{18}$ eV Using the Pierre Auger Observatory. *Physical Review Letters*, **125**, Article ID: 121106.

[160] Abraham, J., Abreu, P., Aglietta, M., Aguirre, C., Allard, D., Allekotte, I., *et al.* (2007) Correlation of the Highest-Energy Cosmic Rays with Nearby Extragalactic Objects. *Science*, **318**, 938-943. https://doi.org/10.1126/science.1151124

[161] Parizot, E. (2004) GZK Horizon and Magnetic Fields. *Nuclear Physics B—Proceedings Supplements*, **136**, 169-178. https://doi.org/10.1016/j.nuclphysbps.2004.10.034

[162] Mollerach, S. and Roulet, E. (2022) Anisotropies of Ultrahigh-Energy Cosmic Rays in a Scenario with Nearby Sources. *Physical Review D*, **105**, Article ID: 063001. https://doi.org/10.1103/physrevd.105.063001

[163] Deason, A.J., Belokurov, V., Koposov, S.E. and Rockosi, C.M. (2014) Touching the Void: A Striking Drop in Stellar Halo Density Beyond 50 kpc. *The Astrophysical Journal*, **787**, Article 30. https://doi.org/10.1088/0004-637x/787/1/30

[164] Hernitschek, N., Cohen, J.G., Rix, H., Sesar, B., Martin, N.F., Magnier, E., *et al.* (2018) The Profile of the Galactic Halo from Pan-STARRS1 3π RR Lyrae. *The Astrophysical Journal*, **859**, Article 31. https://doi.org/10.3847/1538-4357/aabfbb

[165] Helmi, A. (2008) The Stellar Halo of the Galaxy. *The Astronomy and Astrophysics Review*, **15**, 145-188. https://doi.org/10.1007/s00159-008-0009-6

[166] Xue, X., Rix, H., Ma, Z., Morrison, H., Bovy, J., Sesar, B., *et al.* (2015) The Radial Profile and Flattening of the Milky Way's Stellar Halo to 80 kpc from the Segue K-Giant Survey. *The Astrophysical Journal*, **809**, Article 144. https://doi.org/10.1088/0004-637x/809/2/144

[167] Slater, C.T., Nidever, D.L., Munn, J.A., Bell, E.F. and Majewski, S.R. (2016) The Stellar Density Profile of the Distant Galactic Halo. *The Astrophysical Journal*, **832**, Article 206. https://doi.org/10.3847/0004-637x/832/2/206